Journal of ELECTRONIC MATERIALS, Vol. 45, No. 6, 2016
DOI: 10.1007/s11664-016-4347-2

High Piezoelectric Response in $(Li_{0.5}Sm_{0.5})^{2+}$-Modified $0.93Bi_{0.5}Na_{0.5}TiO_3$-$0.07BaTiO_3$ Near the Nonergodic–Ergodic Relaxor Transition

JIWEN XU,[1] QINGLIN LI,[1] CHANGRONG ZHOU,[1,3] WEIDONG ZENG,[1,4] JIANRONG XIAO,[2] JIAFENG MA,[2] CHANGLAI YUAN,[1] GUOHUA CHEN,[1] GUANGHUI RAO,[1] and XUQIONG LI[1]

1.—School of Material Science and Engineering, Guilin University of Electronic Technology, Guilin 541004, Guangxi, People's Republic of China. 2.—College of Science, Guilin University of Technology, Guilin 541004, Guangxi, People's Republic of China. 3.—e-mail: zcr750320@guet.edu.cn. 4.—e-mail: 903286384@qq.com

The $(Bi_{0.5}Na_{0.5})TiO_3$-$BaTiO_3$ system is a promising Pb-free piezoelectric material to substitute for environmentally undesirable Pb-based ferroelectrics. However, understanding the origin of its high piezoelectric response is a fundamental issue that has remained unclear for decades. Here, complex ions $(Li_{0.5}Sm_{0.5})^{2+}$ were introduced to dictate the stability of the electrically-induced ferroelectric state in $0.93(Bi_{0.5}Na_{0.5})_{1-x}(Li_{0.5}Sm_{0.5})_xTiO_3$-$0.07BaTiO_3$ relaxor ceramics. The applied electric field induces a phase transition from a non-ergodic state to a ferroelectric state as well as the realignment of ferroelectric domains. The non-ergodic relaxor state with x = 0–0.02 is accompanied by relatively high piezoelectric activity and the strongest piezoelectricity is observed near the crossover from the nonergodic to the ergodic state. The stable ferroelectric state cannot survive after the removal of the application electric field for the high doping level due to the enhancement of the random field, which is responsible for the rapid decrease of piezoelectric properties for $x > 0.02$ compositions.

Key words: Electroceramics, piezoelectricity, field-induced phase transition

INTRODUCTION

Intensive research on lead-free piezoceramics has been performed in recent years because of increasing environmental and health concerns over the widely used lead-containing $Pb(Zr,Ti)O_3$ (PZT) ceramics.[1] In the past decade, $(1-x)Bi_{0.5}Na_{0.5}TiO_3 - xBaTiO_3$ (BNT-BT) ceramics close to the morphotropic phase boundary (MPB) are among the most promising lead-free piezoelectric materials to compete with PZT due to their enhanced piezoelectric properties.[2–8] Recently, some breakthroughs with ultrahigh $d_{33} \sim 490$ pC/N by constructing rhombohedral–tetragonal phase boundary together with nonstoichiometric sodium for $0.96(K_{0.46}Na_{0.54+x})Nb_{0.95}Sb_{0.05}O_3{}^{-}0.04Bi_{0.5}(Na_{0.82}K_{0.18})_{0.5}ZrO_3$ and $(1-x)(K_{1-y}Na_y)(Nb_{1-z}Sb_z)O_3 - xBi_{0.5}(Na_{1-w}K_w)_{0.5}ZrO_3$ ceramic with x = 0.04, y = 0.52, z = 0.05 and w = 0.18 were reported by Wu et al.[9,10] However, the origin of the piezoelectric property enhancement in lead-free ABO_3 compounds has been a long-standing puzzle which is still being investigated.

Most recent studies on BNT-BT ceramics have attributed the large piezoelectric activity and electric field-induced giant strain to structural phase transition under the application of an electric field.[2,8] However, Maurya et al. demonstrated that electric field-induced structural phase transition is not a prerequisite for achieving high piezoelectric property by comparing with a piezoelectric constant d_{33} in textured and randomly oriented ceramics.[4] In addition, various mechanisms such as monoclinic

(Received August 4, 2015; accepted January 12, 2016; published online February 9, 2016)

bridging phase,[8] nanoscale polar domains,[11–18] incipient piezoelectricity and polarization alignment of polar nanodomains in the nonergodic relaxor have been proposed to explain the structural nature of high piezoelectric activity.[19] Despite long and intensive research about the mechanisms, the underlying origin of the large piezoelectric response cannot be completely understood based on the above mechanisms. Thus, insights into the key structural origin of piezoelectricity are still needed.

As we all know, the as-prepared ferroelectric ceramics must be poled by a strong electric field to realign domains in order to present small-signal piezoelectricity. Meanwhile, the piezoelectric properties are measured on the samples that were previously poled under an electric field and after removing the application poling electrical field. However, most of the reported experimental studies have correlated the piezoelectric properties with the structural and microstructural features in the virgin-state or *in situ* electric field state of the system.[2,4,6,7,20] Such studies failed to offer the crucial information required for a comprehensive understanding of the key structural mechanism of piezoelectricity.

Therefore, in order to fully clarify the microstructural mechanism of the macroscopic piezoelectric behaviors, the characterization of not only the structural features in the virgin-state phase but also the phase transition behaviors companied by the application of a high electric field must be comprehensively studied.

Unlike lead-based ferroelectrics that have varying occupancies on the B-site of an ABO_3 perovskite-type compound, BNT-based ferroelectrics display disorder on the A-site. Generally speaking, the A-sites cation has a stronger interaction with the oxygen anion and hence a change in the A-site cation can perturb the crystal symmetry.[8]

In this study, a BNT-0.07BT composition close to the MPB and the complex ions $(Li_{0.5}Sm_{0.5})^{2+}$ substitution for the A-site were selected as the model system and for modification, respectively. Simple *ex situ* electric field-dependent structural study and electric properties measurements were conducted to investigate the crucial information with regard to the factor which contributes to the anomalous piezoelectric response in $0.93(Bi_{0.5}Na_{0.5})_{1-x}(Li_{0.5}Sm_{0.5})_xTiO_3$-$0.07BaTiO_3$ ceramics.

EXPERIMENTAL

The $0.93(Bi_{0.5}Na_{0.5})_{1-x}(Li_{0.5}Sm_{0.5})_xTiO_3$-$0.07BaTiO_3$ ceramics (BNTLS*x*-BT7, $x = 0$, 0.01, 0.02, 0.03, 0.04 and 0.05) were prepared by a conventional solid-state reaction of $BaCO_3$ (99.5%), Sm_2O_3 (99.0%), Na_2CO_3 (99.0%), Li_2CO_3 (99.0%), Bi_2O_3 (99.5%), and TiO_2 (99.5%). Stoichiometric mixtures were ball-milled with the addition of alcohol for 24 h. After drying at 100°C, the mixtures were calcined at 880°C for 4 h. After the calcination, the mixtures were ball-milled again for 24 h, mixed thoroughly with a PVA binder solution, and then pressed into disk samples (12.0 mm diameter and 1.0 mm thickness) under 100 MPa uniaxial pressure. Following removal of the binder at 600°C for 2 h, the pellets were sintered in an open crucible at 1200°C in air atmosphere for 4 h.

Crystal structures of BNTLS*x*-BT7 ceramics with as-prepared state and prepoled state were detected via x-ray diffractometer (XRD; D8 Advance; Bruker, Germany). Surface microstructures of the ceramics were observed using electron back-scattering diffraction (BES; JSM-5610LV/Noran-Vantage; JEOL, Tokyo, Japan). The surfaces of the disk-shaped specimens were covered with a thin layer of silver paint and fired at 600°C for 30 min. Electrical poling of unpoled samples was completed at room temperature in a silicone oil bath using a constant electric field of 60 kV/cm for 30 min. The direct longitudinal piezoelectric coefficient d_{33} of the poled ceramics was measured after 24 h using a Berlincourt d_{33} meter (ZJ-3A; CAS, Shanghai, China). Dielectric properties were measured using an impedance analyzer (Agilent 4294A; Agilent, Bayan, Malaysia). Temperature-dependent capacitance was measured in a controlled furnace with a heating rate of 2°C/min from 26°C to 250°C. The room-temperature polarization versus electric field hysteresis loops (*P*–*E*) were recorded with a ferroelectric test system (Precision Premier II; Radiant Technologies, Albuquerque, NM, USA) by applying an electric field of triangular waveform at a frequency of 1 Hz. The electromechanical coupling factor, k_p, was determined by the resonance method according to the IEEE Standard using an impedance analyzer (Agilent 4294A).

RESULTS AND DISCUSSION

Figure 1 depicts the composition dependence of the piezoelectric coefficient, d_{33}, and planar electromechanical coupling factor, k_p, of the BNTLS*x*-BT7 ceramics. The d_{33} and k_p exhibit gradual variation with relatively high piezoelectric

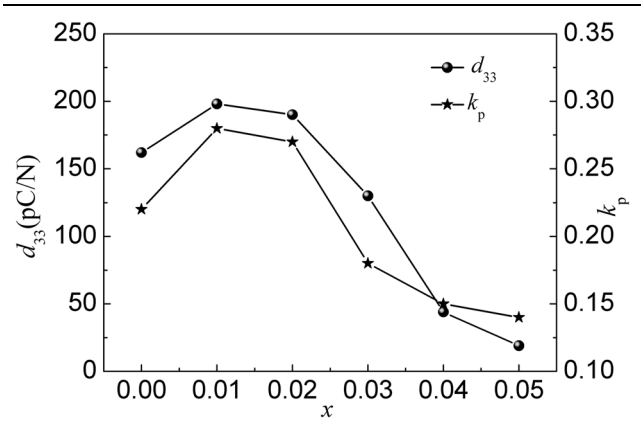

Fig. 1. Piezoelectric constant, d_{33}, and the planar electromechanical coupling factor, k_p, for the BNTLS*x*-BT7 ceramics.

responses in the narrow composition interval of $0 \le x \le 0.02$, peaking at $x = 0.01$ with $d_{33} = 198$ pC/N and $k_p = 0.28$. Subsequently, the piezoelectric properties show a sharp reduction when $x > 0.2$.

It is well known that the crystal structural and the ferroelectric domains largely dictate the piezoelectric performance. In addition, the ferroelectric domain morphology and structure are associated with the crystal structural, dielectric behavior and piezoelectric response. Generally speaking, transition electron microscopy (TEM) is a powerful tool to directly observe domain morphology and structure. However, TEM observation requires very delicate sample preparation. Thus, in the process of TEM sample preparation, the structural changes could be induced by mechanical loading due to polishing and dimpling, or even during ion-milling. Furthermore, the domain morphology and size cannot be formed uniformly throughout the thinner and thicker parts of the TEM samples, as it would be more of a surface effect.[21,22] As a consequence, the structural analyses may in some cases contradict the results from different groups.[5,7,23–25] Recently, some researchers reported the composition dependence of the domain morphology and the crystal structure as well as their correlation with the dielectric behavior on a BNT-BT system.[26,27] They established a clear relationship between domain morphology and dielectric frequency dispersion in the frequency range of 1–100 kHz: nanodoamains correspond to a strong frequency dispersion while large domains show a weaker frequency dependence.[27] Therefore, the domain evolution can be characterized by the dielectric spectrum.

Figure 2 presents the temperature dependences of the dielectric permittivity of unpoled and poled BNTLSx-BT7 ceramics for three measurement frequencies: 1 kHz, 10, kHz, and 100 kHz. In the spectra of all the unpoled specimens, a strong frequency-dependent dispersion from room temperature up to 250°C was observed, which categorizes all the materials as relaxor ferroelectrics. However, a clear change for poled $x < 0.02$ samples in the low-temperature region with a relatively weak

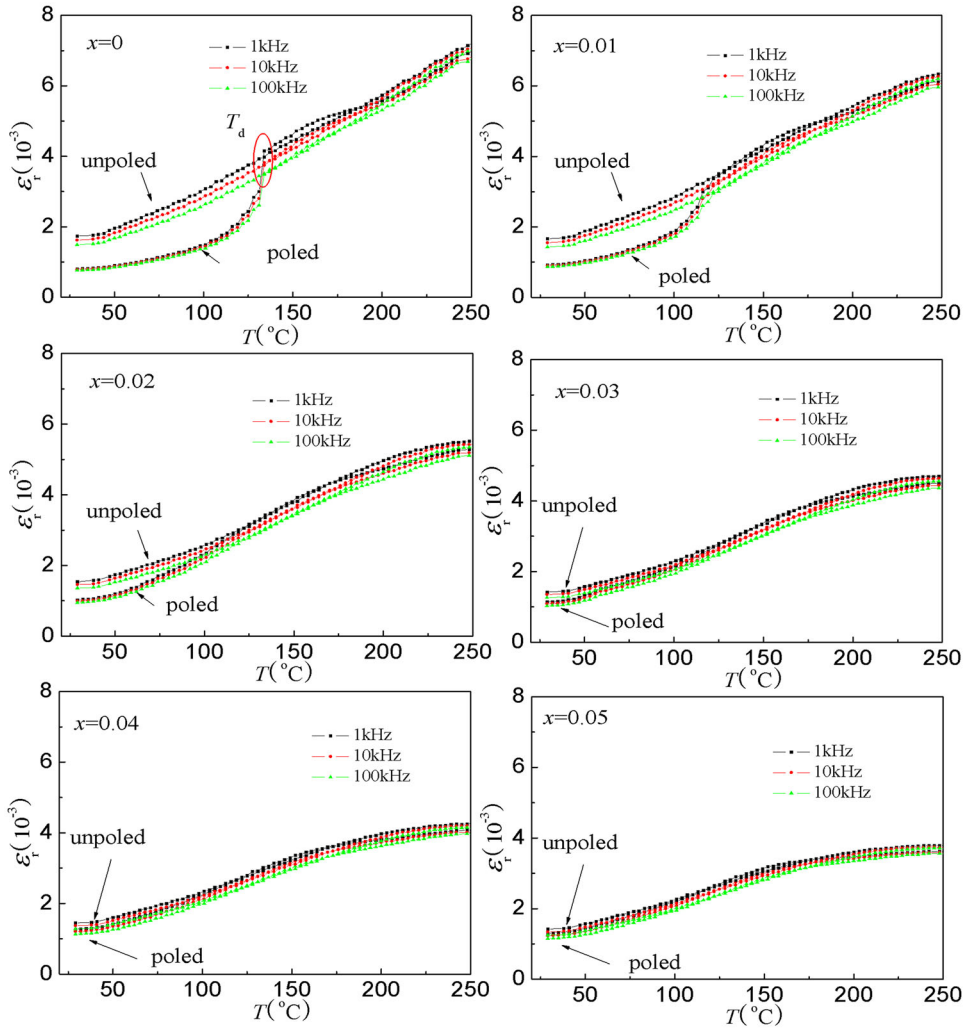

Fig. 2. Temperature dependence of dielectric constant, ε_r, for the unpoled and poled BNTLSx-BT7 ceramics.

frequency-dependent dispersion and decreasing dielectric permittivity takes place. It is suggested that BNTLS*x*-BT7 ceramics with $x < 0.02$ are in a nonergodic relaxor ferroelectrics state undergoing a field-induced phase transition to a long-range ordered state, which is consistent with the previous results of BNT-BT ceramics.[28,29] This means that the initially nanoscale polar regions are triggered to grow into micron-sized domains or ordered reorientation with the application of an electric field. It is also interesting to note that the frequency-dependent dispersion and dielectric permittivity for unpoled and poled specimens with $x > 0.02$ show only slight variation. This indicates that the BNTLS*x*-BT7 ceramics with $x > 0.02$ are ergodic relaxor ferroelectrics.

As a result, this demonstrates that the high piezoelectric response can be obtained near the nonergodic–ergodic relaxor transition. Both theoretical and experimental studies indicate that the piezoelectric responses are enhanced by reducing the domain size down to nanoscale domain due to the instability of the nanodomains with low wall energy.[11–14] On the other hand, the piezoelectric properties are only obtained by the poling electric field inducing the percolation correlation-ordered domains. In addition, the correlation-ordered polarization state cannot be established by the application with a sufficiently high electric field when the nanodomain size decreases to a critical value. Thus, it is natural to infer that the nonergodic–ergodic relaxor transition point, meaning the critical nanodomain size, presents the largest piezoelectric activity due to the minimum domain size that can also establish the correlation-ordered state. Therefore, the excellent piezoelectricity of the materials has been attributed to the onset of the ergodic relaxor state. On the other hand, it has been reported that grain size greatly affects the extrinsic contributions to piezoelectricity. Fine-grained

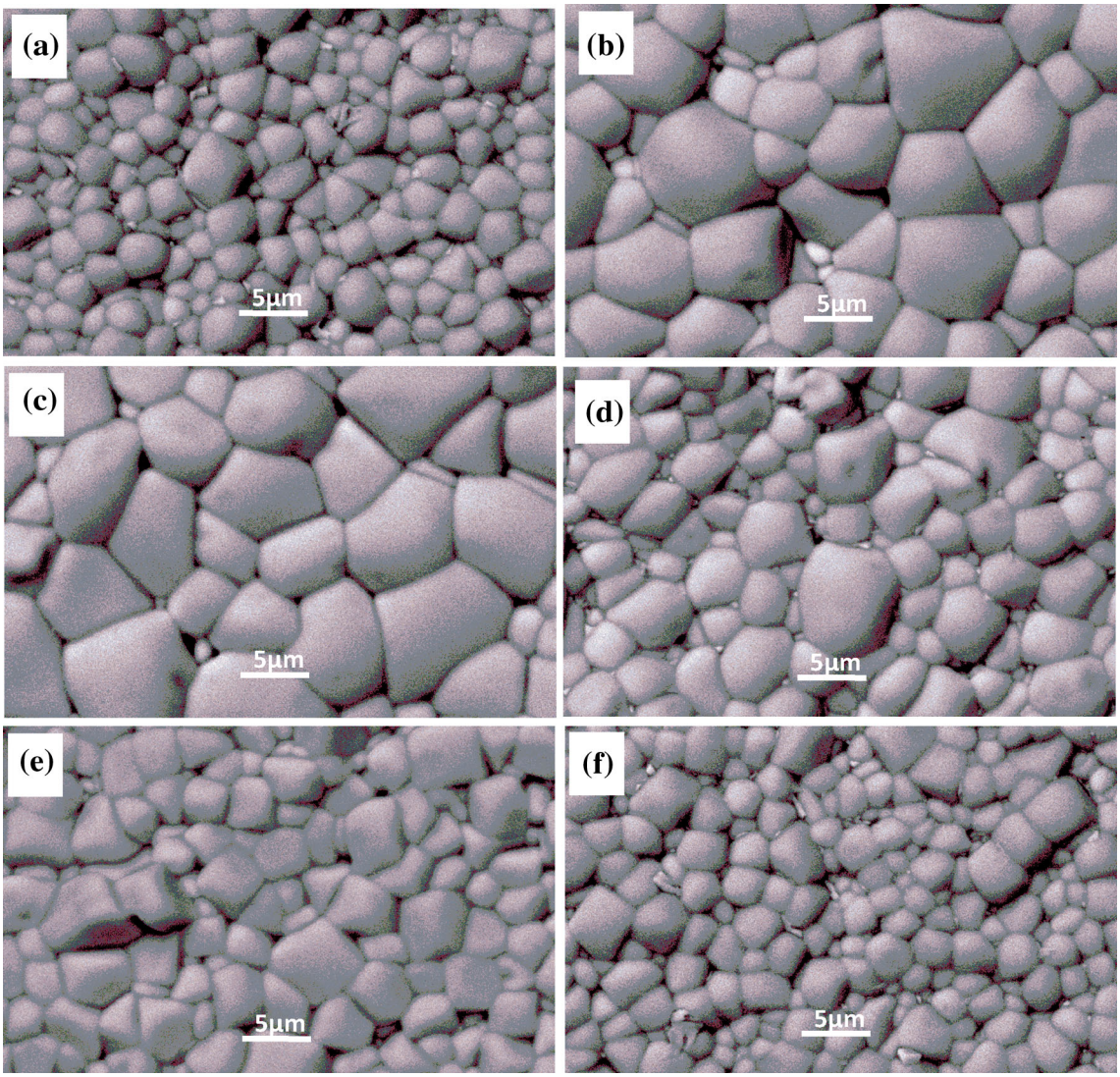

Fig. 3. SEM micrographs of BNTLS*x*-BT7 ceramics. (a) $x = 0$; (b) $x = 0.01$; (c) $x = 0.02$; (d) $x = 0.03$; (e) $x = 0.04$; and (f) $x = 0.05$.

ceramics have limited domain variants and the domain reorientation is hindered by strong coupling between grain boundaries and domain walls, leading to lower polarization and piezoelectric response.[30,31] Figure 3 displays the scanning electron microscope (SEM) images with BES of BNTLSx-BT7 ceramics. Clearly, the grain size first increases and then decreases with x, which is consistent with the variation trend of piezoelectric properties of BNTLSx-BT7 ceramics. The depoling behaviors with temperature dependent electromechanical coupling factor, k_p, of BNTLSx-BT7 ceramics are presented in Fig. 4, from which it can be seen that the depoling temperature, T_d, decreases evidently with increasing x. This can contribute to the decrease in the degree of nonergodicity, which gives rise to metastablity of the field-induced orientation domains.

It is well known that dopant ions of ferroelectrics are often intended to generate new functionalities or enhance the already existing properties by inducing local structure distortion and random electric field variation. Differently charged ions randomly distributed over equivalent crystallographic positions are considered as the origin of quenched random electric fields.[32–36] At the same time, the random nanostress due to ionic volume constraints is another important source of random electric field.[32,33] Due to the enhancement of random electric fields with the concentration of foreign $(Li_{0.5}Sm_{0.5})^{2+}$ ions in BNTLSx-BT7 ceramics, an initial non-ergodic state renders an ergodic state; thus, the degree of non-ergodicity may decrease. Therefore, the formation of long-range order is impeded and the reversible character of the electric field-induced phase transition linked to the ergodic state is increased and thus there coexists both the non-ergodic phase and the ergodic phase at x = 0–0.03. The room-temperature polarization versus electric field hysteresis loops (P–E) are shown in Fig. 5. The polarization hysteresis loops display typical square loops for x = 0 and 0.01 ceramics. However, the polarization hysteresis loops start to deviate from their square shape with a constriction developing, leading eventually to slim loops with increasing x. The reduced remnant polarization, P_r, and coercive field, E_C, with x implies weakening ferroelectricity. From the results in Figs. 2 and 5, it is demonstrated that the BNTLSx-BT7 ceramics undergo a transition from the non-ergodic state and ergodic phase with increasing x.

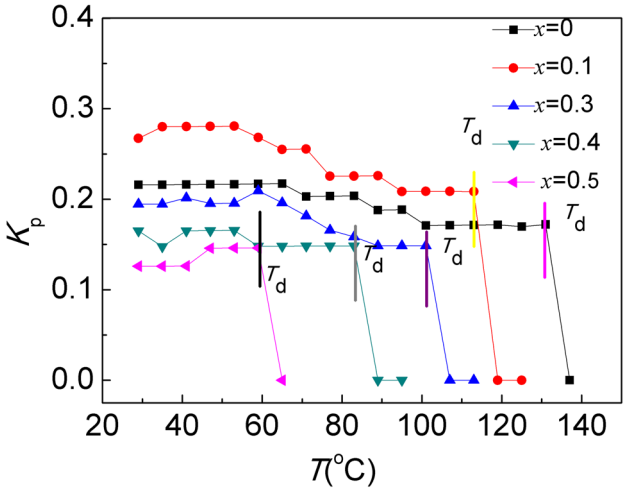

Fig. 4. Temperature dependence of electromechanical coupling factor k_p for BNTLSx-BT7 ceramics.

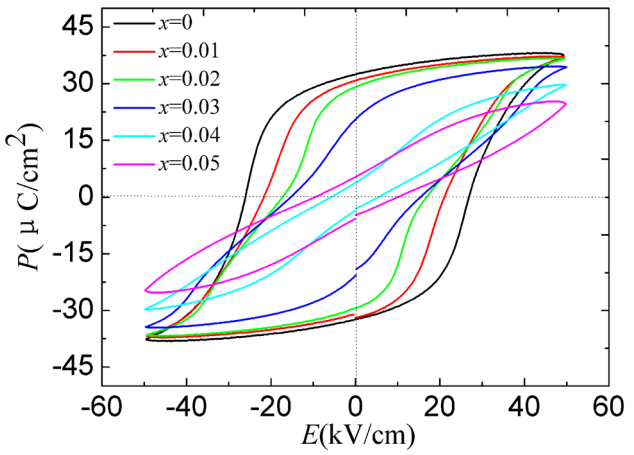

Fig. 5. P–E loops of the BNTLSx-BT7 ceramics at room temperature.

Owing to the fact that the non-ergodic to ergodic state crossover is always accompanied by structure transition, the XRD patterns of the unpoled and poled BNTLSx-BT7 ceramics were conducted and are shown in Fig. 6. The unbiased structure determined via XRD is pseudocubic with a narrow reflection and virtually non-cubic distortion due to the piezoelectricity and the broadening at the root of the peaks, which is in agreement with the XRD patterns of the previously reported BNT-BT system.[24,28] The appearance of intensity in the diffraction patterns with a macroscopically pseudocubic structure can be the result of coherence effects of nanodomains.[37,38]

The next investigation was aimed to determine how and to what extent the poling electric field influences the structure of the BNTLSx-BT7 ceramics. Drastic differences are observed due to a field-induced phase transition into a long-range ordered state. The XRD patterns of the $x \leq 0.02$ poled pellets exhibit obvious splitting 002/200 peaks, suggesting that the application electric field induced the structural transition from pseudocubic phase to tetragonal symmetry. However, the relative intensities of the peaks are different from different compositions, e.g., the ratio between the intensities of the 002 and 200 tetragonal peaks has been changed, which is common when the domains are switched in order to orientate in accordance with an external field. When $x > 0.02$, the obscure splitting peaks indicate weak

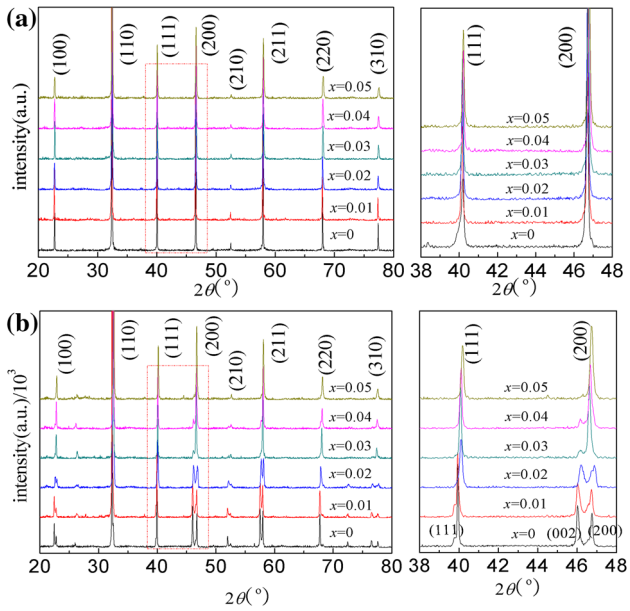

Fig. 6. XRD pattern of the unpoled and poled BNTLS*x*-BT7 ceramics: (a) unpoled samples and (b) poled samples.

tetragonal distortion, which is in agreement with the results of dielectric spectra. In Fig. 6, it is indicated that the tetragonal-pseudocubic phase transition may be responsible for the enhanced piezoelectric properties.

Along with the electric field, two types of domain switching corresponding to the phase transition may be activated in relaxor ferroelectrics. First, the nanodomains may coalesce into micron-sized domains by merging neighboring nanodomains, a concomitantly electric field-induced phase transition. Similar nanodomains coalescence associated with the formation of the long-range ferroelectric domains has been found in the BNT-BT system and the Sc-doped $Pb(Mg_{1/3}Nb_{2/3})O_3$ ceramics.[16,39] Second, the application of electric field results in the redistribution of an invariant nanodomain population with a strong percolation-correlated polar state. The same results have been reported in $Pb(Mg_{1/3}Nb_{2/3})O_3$-$PbTiO_3$ crystals.[40] When the strong correlation-ordered nanodomains persist after removing the external field, and their sizes are larger than the coherence length of diffraction radiation, the smeared natural average symmetry of bulk ceramics due to the nanodomains adaptive peak reappears. The average effect in the x-ray diffraction of ordered nanodomains leads to the observed XRD patterns of the electric field-induced phase transition, which is similar to the adaptive diffraction phase. It should be noted that the strong correlation-ordered nanodomains are not microdomains in the usual thermodynamic sense. As a result, the ordered nanodomains are broken into a random state when the temperature increases to depolarization temperature (T_d), as shown in Fig. 2a, e.g., the strong frequency-dependent dispersion reappears. On lowering the temperature to room temperature after thermal treatment above T_d for the prepoled samples, the strong frequency-dependent dispersion is almost the same as the unpoled samples, suggesting that they cannot coalesce into larger entities. It is therefore of fundamental importance to investigate the interrelationship between the polarization alignment/domains reorientation and phase transition during the poling process. Further work in this direction is in progress.

The discovery presented here reveals a new driving mechanism for the high piezoelectric response of relaxor ferroelectrics, and should be helpful in searching for new lead-free piezoelectric materials with ultrahigh performance.

CONCLUSIONS

The mechanism explaining the high piezoelectric properties in BNTLS*x*-BT7 ceramics was investigated. It is demonstrated that the content of dopant ions of $(Li_{0.5}Sm_{0.5})^{2+}$ greatly affects the degree of nonergodicity of lead-free relaxor BNTLS*x*-BT7 ceramics. The increased content of $(Li_{0.5}Sm_{0.5})^{2+}$ ions enhances the quenched random electric field, and consequently induces a nonergodic relaxor state toan ergodic relaxor state transition. The electric field-induced nonergodic to ferroelectric state crossover as well as phase transition from the pseudocubic structure to tetragonal phase is associated with relatively high piezoelectric properties. The high piezoelectric activity could occur near the nonergodicity to ergodicity transition. The competition between non-reversible and reversible nanodomains reorientation are suggested to be the primary contributing factors to the excellent piezoelectricity in this newly developed BNTLS*x*-BT7 relaxor ceramics. Furthermore, the obtained results give the necessary microscopically insight into the driving mechanism of the large piezoelectric response.

ACKNOWLEDGEMENT

Part of this work was financially supported by the National Nature Science Foundation of China (11564007, 61561015, 61361007 and 51462005) and Guangxi Key Laboratory of Information Materials (1310001-Z) and the Natural Science Foundation of Guangxi (Grants Nos. 2012GXNSFGA60002 and 2015GXNSFAA 139250).

REFERENCES

1. J. Rödel, W. Jo, K.T.P. Seifert, E.-M. Anton, T. Granzow, and D. Damjanovic, *J. Am. Ceram. Soc.* 92, 1153 (2009).
2. H. Simons, J.E. Daniels, J. Glaum, A.J. Studer, J.L. Jones, and M. Hoffman, *Appl. Phys. Lett.* 102, 062902 (2013).
3. W. Jo, S. Schaab, E. Sapper, L.A. Schmitt, H.-J. Kleebe, A.J. Bell, and J. Rödel, *J. Appl. Phys.* 110, 074106 (2011).
4. D. Maurya, A. Pramanick, K. An, and S. Priya, *Appl. Phys. Lett.* 100, 172906 (2012).
5. S.T. Zhang, A.B. Kounga, E. Aulbach, T. Granzow, W. Jo, H.J. Kleebe, and J. Rödel, *J. Appl. Phys.* 103, 034107 (2008).
6. R. Ranjan and A. Dviwedi, *Solid State Commun.* 135, 394 (2005).

7. C. Ma, H. Guo, and X. Tan, *Adv. Funct. Mater.* 23, 5261 (2013).
8. D. Maurya, M. Murayama, A. Pramanick, W.T. Reynolds Jr, K. An, and S. Priya, *J. Appl. Phys.* 113, 114101 (2013).
9. J. Wu, D. Xiao, and J. Zhu, *Chem. Rev.* 115, 2559 (2015).
10. X. Wang, J. Wu, D. Xiao, J. Zhu, X. Cheng, T. Zheng, B. Zhang, X. Lou, and X. Wang, *J. Am. Chem. Soc.* 136, 2905 (2014).
11. T. Sluka, A.K. Tagantsev, D. Damjanovic, M. Gureev, and N. Setter, *Nat. Commun.* 3, 748 (2012).
12. L.-F. Wang and J.-M. Liu, *Appl. Phys. Lett.* 91, 092908 (2007).
13. R. Ahluwalia, T. Lookman, A. Saxena, and W. Cao, *Phys. Rev. B* 72, 014112 (2005).
14. R. Theissmann, R.L.A. Schmitt, J. Kling, R. Schierholz, K.A. Schönau, H. Fuess, M. Knapp, H. Kungl, and M.J. Hoffmann, *J. Appl. Phys.* 102, 024111 (2007).
15. Y.M. Jin, Y.U. Wang, and A.G. Khachaturyan, *J. Appl. Phys.* 94, 3629 (2003).
16. H. Guo, C. Ma, X. Liu, and X. Tan, *Appl. Phys. Lett.* 102, 092902 (2013).
17. D. Xue, Y. Zhou, J. Gao, X. Ding, and X. Ren, *EPL* 100, 17010 (2012).
18. J. Fu, R. Zuo, and Z. Xu, *Appl. Phys. Lett.* 99, 062901 (2011).
19. H.-S. Han, W. Jo, J.-K. Kang, C.-W. Ahn, I.W. Kim, K.-K. Ahn, and J.-S. Lee, *J. Appl. Phys.* 113, 154102 (2013).
20. H. Simon, J. Daniels, W. Jo, R. Dittmer, A. Studer, M. Avdeev, J. Rödel, and M. Hoffman, *Appl. Phys. Lett.* 98, 082901 (2011).
21. L.A. Schmitt, K.A. Schönau, R. Theissmann, H. Fuess, H. Kungl, and M.J. Hoffmann, *J. Appl. Phys.* 101, 074107 (2007).
22. M. Otoničar, S.D. Škapin, B. Jančar, and D. Suvorov, *J. Appl. Phys.* 113, 024106 (2013).
23. C. Ma, H. Guo, S.P. Beckman, and X. Tan, *Phys. Rev. Lett.* 109, 107602 (2012).
24. J.E. Daniels, W. Jo, J. Rödel, and J.L. Jones, *Appl. Phys. Lett.* 95, 032904 (2009).
25. B.W.-V. Eerd, D. Damjanovic, N. Klein, N. Setter, and J. Trodahl, *Phys. Rev. B* 82, 104112 (2010).
26. W. Ge, C. Luo, C.P. Devreugd, Q. Zhang, Y. Ren, J. Li, H. Luo, and D. Viehland, *Appl. Phys. Lett.* 103, 241914 (2013).
27. C. Ma, X. Tan, E. Dul'Kin, and M. Roth, *J. Appl. Phys.* 108, 104105 (2010).
28. R. Garg, B.N. Rao, A. Senyshyn, P.S.R. Krishna, and R. Ranjan, *Phys. Rev. B* 88, 014103 (2013).
29. W. Zeng, X. Zhou, J. Chen, J. Liao, C. Zhou, Z. Cen, T. Yang, H. Yang, Q. Zhou, G. Chen, and C. Yuan, *Appl. Phys. Lett.* 104, 242910 (2014).
30. C.A. Randall, N. Kim, J.-P. Kucera, W. Cao, and T.R. Shrout, *J. Am. Ceram. Soc.* 81, 677 (1998).
31. C. Zhou, Z. Cen, H. Yang, Q. Zhou, W. Li, C. Yuan, and H. Wang, *Phys. B* 410, 13 (2013).
32. W. Kleemann, *J. Adv. Dielect.* 2, 1241001 (2012).
33. W. Kleemann, *Phys. Status Solidi B* 251, 1993 (2014).
34. D. Gobert, R. Dittmer, J. Rödel, V.V. Shvartsman, and D.C. Lupascu, *J. Am. Ceram. Soc.* 97, 3904 (2014).
35. A.A. Bokov and Z.-G. Ye, *J. Mater. Sci.* 41, 31 (2006).
36. R. Dittmer, D. Gobeljic, W. Jo, V.V. Shvartsman, D.C. Lupascu, J.L. Jones, and J. Rödel, *J. Appl. Phys.* 115, 084111 (2014).
37. Y.M. Jin, Y.U. Wang, and A.G. Khachaturyan, *Phys. Rev. Lett.* 91, 197601 (2003).
38. K.A. Schönau, L.A. Schmitt, M. Knapp, H. Fuess, R.-A. Eichel, H. Kungl, and M.J. Hoffmann, *Phys. Rev. B* 75, 184117 (2007).
39. W. Qu, X. Zhao, and X. Tan, *J. Appl. Phys.* 102, 084101 (2007).
40. Y. Sato, T. Hirayama, and Y. Ikuhara, *Phys. Rev. B* 107, 187601 (2011).